Effect of cavity length on stimulated emission from Fabry-Pérot Gunn lasers

A. Agarwal, S. Chung, and N. Balkan[a)]
Department of Electronic Systems Engineering, University of Essex, Colchester CO4 3SQ, United Kingdom

G. Hill
National Centre for III-V Technologies, University of Sheffield, Mappin Street, Sheffield S1 3JD, United Kingdom

(Received 7 July 2006; accepted 3 November 2006; published online 12 January 2007)

Emission characteristics from GaAlAs–GaAs–GaAlAs Gunn devices of different lengths placed in Fabry-Pérot cavities have been investigated. The emission from the device of length of 194 μm is stimulated in nature, whereas for the other two devices of lengths of 100 and 50 μm, the emission is spontaneous. Lasing action in such devices, when biased above the threshold of negative differential resistance, arises from the band to band recombination of impact-ionized nonequilibrium electron hole pairs created within the propagating high field Gunn domains. Quantitative results evaluated using nonequilibrium semiconductor-statistics show that reduction in the length of the device leads to (a) a shift of the gain peak towards higher energies and (b) an increase in the average nonequilibrium carrier temperature. As a result, lasing in very short devices is inhibited and only ultra-bright-spontaneous emission is observed. © *2007 American Institute of Physics*.
[DOI: 10.1063/1.2409311]

I. INTRODUCTION

Spontaneous light emission from propagating high field domains in a long ($L \approx 1$ mm) GaAs Gunn device was first reported by Southgate.[1] Southgate also showed that when the pulse current through the device (0.5 mm length) was only slightly above the critical value for ionization, the spectrum of the recombination radiation was essentially that of spontaneous emission and when the pulse current was increased gradually, a threshold level was reached where the spectrum showed large erratic spikes (stimulated emission) in the output.[2] Gelmont and Shur[3] and Sudzilovskii[4] studied the correlations for stimulated emission concluding that the population inversion of excess carriers can be reached in Gunn diodes with lengths of $L \geqslant 0.5$ mm, irrespective of the doping (background) electron density, when the applied field is about 12-fold excess over the Gunn effect threshold field. Arutyunyan and Varosyan[5] calculated the effect of electron density and the length of the device on the stimulated emission conditions. Recently, we have shown that the spontaneous emission characteristics from Gunn devices are controlled by the applied field, temperature, and device dimensions,[6,7] and also predicted that spontaneous emission from GaAs Gunn device may evolve into stimulated emission when it is placed in a Fabry-Pérot[8,9] or vertical microcavity.[10] The operation of a Fabry-Pérot and vertical cavity surface-emitting (VCSE) Gunn lasers has been demonstrated recently.[11] In the Fabry-Pérot lasers the length of the Gunn device was varied from 213 μm to 1 mm.

In this paper, our aim is to study the emission characteristics from the Gunn devices with cavity lengths shorter than those studied previously to establish a threshold cavity length required for enough gain without significantly disturbing the nonequilibrium carrier distribution by excessive carrier heating.

II. EXPERIMENT

The Fabry-Pérot devices used in the experiments are grown by metal-organic chemical vapor deposition (MOCVD) on a semi-insulating GaAs substrate and consists of an $n = 4.8 \times 10^{17}$ cm^{-3} doped GaAs active layer (thickness = 1 μm) sandwiched between the $Al_xGa_{1-x}As$ ($x = 0.32$) waveguiding (WG) layers. The details about WG layer and device structure together with contact configuration are shown in Fig. 1(a).Modified "dumbbell" shape [Fig. 1(b)] samples were used for the investigation as they were found to be more stable at high fields.[9] The samples with 194 μm in length were cleaved and the rest of the samples were dry-etched perpendicular to the current flow direction to define two mirror facets. No reflective coating was used on the facets. Three devices having dimensions (length × width) of 194×200, 100×20, and 50×20 μm^2 were investigated.

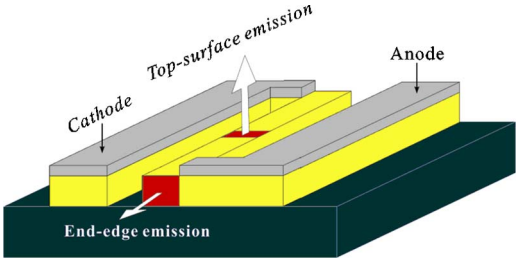

FIG. 1. Schematic diagram of a modified dumbbell Gunn device (a three-dimensional view).

[a)]Electronic mail: balkan@essex.ac.uk

The devices were placed onto ceramic holders for good electrical insulation and mounted on a copper heat sink in a liquid nitrogen cryostat with optical windows. In order to minimize Joule heating, voltage pulses of duration of 80 ns were applied along the devices with a duty cycle of $8\times10^{-5}-1.5\times10^{-4}$. The applied electric field was determined from the voltage drop between the electrodes. The current through the devices was determined from the voltage drop across a 50 Ω resistor placed in series with the device. The emitted light from the device was collected by an antireflective lens and dispersed using a 1/3 m monochromator (Bentham, M300EA, 830 grooves/mm) and was detected using a cooled GaAs photomultiplier (Hamamatsu, R1767). The data were averaged and captured using a digital oscilloscope (Tektronix, TDS 2012) with a bandwidth of 100 MHz. All the measurements comprising of current density–electric field (*J-F*) characteristics, electroluminescence intensity–electric field (*L-F*) characteristics, and electroluminescence (EL) spectra were carried out at 90 K.

III. RESULTS

EL spectrum for the device of length of 194 μm together with *J-F* and *L-F* characteristics is shown in Figs. 2(a) and 2(b). It is evident from Fig. 2(a) that emission from the device starts at 3 kV/cm and emitted power intensity increases rapidly with increase in applied electric field. This field corresponds nearly to the onset of impact ionization from the high fields of the traveling Gunn domains as also evident from the sudden increase in the current.[6,8] The lasing spectrum of the waveguided Gunn device is plotted in Fig. 2(b) for an applied electric field of 3.8 kV/cm with pulse width of 80 ns. The dominant mode is accompanied by some other modes.[12] The wavelength for the dominant mode is 845 nm and the half width is about 0.7 nm (the resolution of the monochromator). The lasing action arises from the recombination of nonequilibrium electrons and holes produced by impact ionization within the traveling high field domain. It is important to note that when the applied field or the pulse width or the temperature was increased, then the emission spectrum shows erratic mode jumping behavior due to Joule heating of the device. In our setup we used a ceramic holder. For stable operation it is important to improve on the thermal management.

The EL spectrum for the device of length of 100 μm is shown in Fig. 3. This spectrum shows that the emission is spontaneous in nature and the full width at half maximum (FWHM) is 50 nm. The EL spectrum for the device of length of 50 μm is shown in Fig. 4, which also shows that the emission is of spontaneous nature and the FWHM is 46 nm. We increased the pulse width up to 120 ns but still the emission was spontaneous. The EL emission intensity increased with increasing the applied electric field, and some spectral narrowing was observed for these two devices but no lasing spikes were observed. This narrowing may be associated with self absorption and cavity effects. Therefore, it is observed that lasing occurs for the device of length of 194 μm only, indicative of the fact that the dimensions may play a significant role for observing lasing.

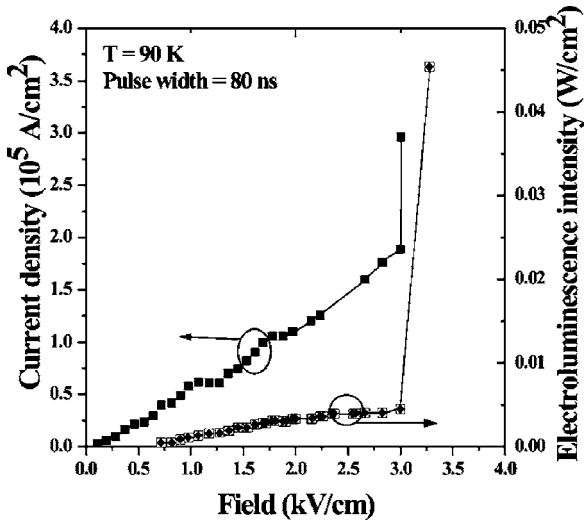

(a)

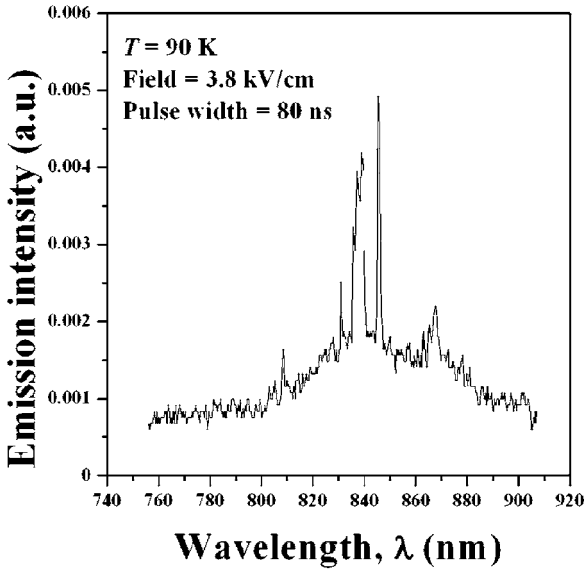

(b)

FIG. 2. (a) Current density–electric field (*J-F*) and top-surface electroluminescence intensity–electric field (L-F) characteristics for the device of length of 194 μm. (b) End-edge electroluminescence spectrum for the device of length of 194 μm.

IV. DISCUSSION

A. Domain dynamics and photon accumulation

In a Gunn device, a space-charge domain is nucleated at applied electric fields beyond the negative differential resistance (NDR) threshold.[8] The space-charge domain with a high built-in field moves from cathode to anode longitudinaly across the device.[13] Excess carriers are created within the domain due to the field-induced impact ionization.[14] At a given point in the device left after the transit of the initiating domain, the excess carriers recombine at a rate corresponding to the band-to-band recombination and the consecutive domains may travel through the device and pass through the same point creating further excess carriers.[1] In the derivation of the related expressions, we assumed the following conditions.

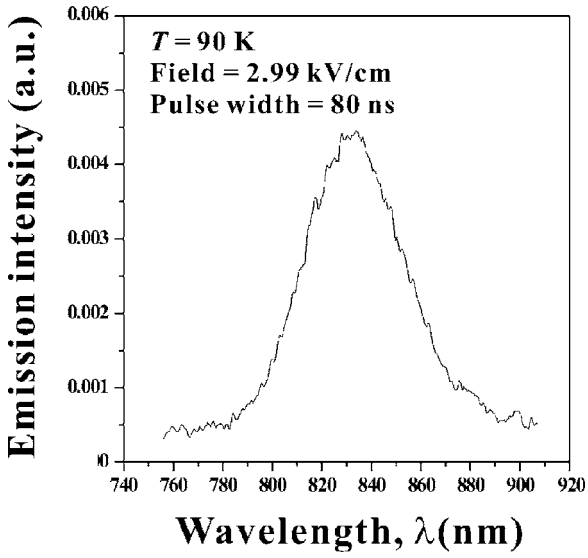

FIG. 3. End-edge electroluminescence spectrum for the device of length of 100 μm.

(i) The initial excess carrier density is $n_{ex}(0)$ and the background doping density at any point is n_0.
(ii) The sample thickness d is much larger than light wavelength λ, therefore the interference effects of the light due to inner reflections are negligible.
(iii) The excess carriers are generated uniformly throughout the sample and those that are generated during one domain transit do not change the field distribution in the following domain, and hence impact ionization rate is constant for all domains in transit.
(iv) The surface recombination is neglected and the number of traps is assumed to be negligible or there is no differential trapping of electrons and holes, therefore excess electron and hole densities at any given time are equal: $n_{ex}=p_{ex}$.

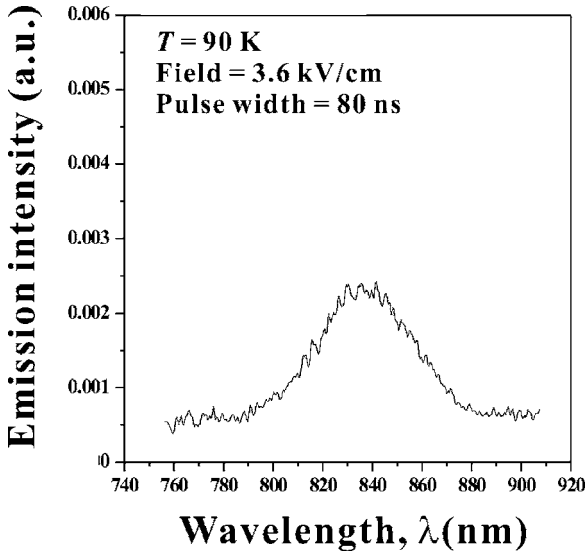

FIG. 4. End-edge electroluminescence spectrum for the device of length of 50 μm.

By using a few well-known equations,[15] we can quantitatively derive a survival ratio of the excess carriers. The survival ratio R_A at a given point A along the device is defined as the ratio of the excess carrier to the intrinsic carrier density during one domain transit and reflects the excess carrier accumulation.

$$R_A = \frac{n_{ex}(t > t_{tr})}{n_{ex}(0)}, \tag{1}$$

where n_{ex} is the excess carrier density and t_{tr} is the domain transit time. We do this by calculating the time dependence of the excess carrier density. The time-dependent excess carrier density is as follows:

$$n_{ex} = n_{ex}(0) \quad \text{at } t \leqslant t_{tr}, \tag{2a}$$

$$\frac{dn_{ex}}{dt} = -\frac{n_{ex}}{\tau} \quad \text{at } t > t_{tr}, \tag{2b}$$

where $n_{ex}(0)$ is the initial excess carrier density generated by impact ionization for the first domain transit and τ is the recombination lifetime. Equations (2a) and (2b) represent the initial condition and the rate of change of excess carrier density, respectively. Equation (2b) solved at a time t_{tr} is

$$n_{ex}(t_{tr}) = n_{ex}(0)\exp\left(-\frac{t_{tr}}{\tau}\right). \tag{3}$$

Therefore, Eq. (3) represents the transient carrier density after the transit of the first domain and when second domain arrives at the point. The bulk recombination rate U depends nonlinearly on the excess carrier density. U can be written as[16]

$$U = A(n - n_0) + B(pn - p_0n_0) + C_p(p^2n - p_0^2n_0) + C_n(pn^2 - p_0n_0^2), \tag{4}$$

where $n=n_0+n_{ex}$ and $p=p_0+p_{ex}$. n_0 and p_0 indicate the background electron and hole densities, respectively. From our assumption $n_{ex}=p_{ex}$. It allows Eq. (4) to be simplified to

$$U \approx An_{ex} + B(p_0 + n_0 + n_{ex})n_{ex} + C_p(p_0^2 + 2p_0n_{ex} + {n_{ex}}^2)n_{ex} + C_n(n_0^2 + 2n_0n_{ex} + {n_{ex}}^2)n_{ex}. \tag{5}$$

The recombination lifetime is defined as

$$\tau = n_{ex}/U. \tag{6}$$

From Eqs. (5) and (6), τ becomes

$$\tau \approx [A + B(p_0 + n_0 + n_{ex}) + C_p(p_0^2 + 2p_0n_{ex} + {n_{ex}}^2) + C_n(n_0^2 + 2n_0n_{ex} + {n_{ex}}^2)]^{-1}. \tag{7}$$

The second term, indicating the radiative recombination lifetime τ_r, is[17]

$$\tau_r = [B(p_0 + n_0 + n_{ex})]^{-1}, \tag{8}$$

where the radiative recombination coefficient is $B=2.1\times10^{-9}$ cm^2/s at $T=90$ K,[18] the background hole density is $p_0=1.79\times10^6$ cm^{-3},[19] and the background electron density is $n_0=4.8\times10^{17}$ cm^{-3}. In the calculating τ_r value, we simply

TABLE I. Survival rate of excess carriers calculated with the recombination time $\tau=5\times10^{-10}$ s at $T=90$ K.

Device length L (μm)	Transit frequency $f_T=v_d/L$ ($\times10^9$ Hz)	Domain transit time $t_{tr}=1/f_T$ (ns)	Survival rate of excess carriers S
194	1.3	0.76	0.16
100	2.6	0.39	0.39
50	5.1	0.2	0.62

took $n_{ex}=n_{ex,th}=6.7\times10^{17}$ cm^{-3}, where $n_{ex,th}$ is the excess carrier density at lasing threshold at 90 K, as described in the next section. In fact, τ_r will depend strongly on n_{ex} which is time dependent making the theory difficult to handle analytically. From Eq. (8) the radiative recombination lifetime at 90 K is then calculated to be $\tau_r=5\times10^{-10}$ s.

The domain transit time, t_{tr} in Eq. (3), is given by

$$t_{tr}=L/v_d, \tag{9}$$

where L is the length of the device and v_d is the saturation electron drift velocity. (For our samples these values are $L=50$, 100, and 194 μm and $v_d=2.556\times10^7$ cm/s at $F=3.8$ kV/cm at $T=90$ K). The saturation electron drift velocity was obtained by the Monte Carlo method as described by us elsewhere.[20] Substituting the domain transit time into Eq. (3) we finally evaluated survival ratios $[n_{ex}(t>t_{tr})]/n_{ex}(0)$ of Eq. (1). It is noted in Table I that carrier accumulation is more effective in the case of the shorter length device.

In addition to the survival rate the impact ionization and domain repetition are also critical in evaluating the excess carrier density. With the assumption of a constant ionization rate during a domain transit, the excess carrier density n_{ex} is given by[14]

$$n_{ex}=\int_0^L n_0(x)\alpha_e dx, \tag{10}$$

where n_0, α_e, and L are the background electron density, impact ionization coefficient, and the device length, respectively. For a device operated by a pulse width longer than the domain transit time, a multiplicative factor γ, representing a multiplication term of the domain repetition rate (f_T) and the pulse width (t_{pulse}), should be taken into account with the survival rate of $\exp(-t_{tr}/\tau)$. Then n_{ex} is given as

$$n_{ex}=n_0\alpha_e L\gamma\exp(-t_{tr}/\tau). \tag{11}$$

Above the NDR threshold, the domain field increases rapidly with applied voltage and may exceed the threshold field for the impact ionization, $F_{II}\approx100$ kV/cm even by infinitesimal increase in the applied voltage.[20] Therefore it is not realistic to determine the impact ionization coefficient by the well-known relationship between the ionization coefficient and electric field. Instead we use an indirect empirical method for the determination of α_e from the lasing threshold conditions. When losses in the cavity are taken into account the threshold gain required for the lasing condition, $\langle g\rangle_{th}$, can be obtained as follows:[21]

$$\Gamma\langle g\rangle_{th}=\alpha_i+(1/L)\ln(1/r_1r_2), \tag{12}$$

where the average internal loss of a cavity is $\alpha_i\approx10$ cm^{-1} and the mean mirror intensity reflection coefficient for GaAs-air interface is $R=r_1r_2\approx0.32$. Taking the optical confinement $\Gamma=1$ and the cavity length of the device exhibiting lasing in our experiment, $L=194$ μm, we find the lasing threshold gain $\langle g\rangle_{th}=69$ cm^{-1}. Using the standard gain model as described in the next section the threshold excess carrier density for lasing in the sample with $L=194$ μm is evaluated to $n_{ex,th}$ (194 μm)$=6.7\times10^{17}$ cm^{-3}, and then the ionization coefficient $\alpha_e=4.3$ cm^{-1} from Eq. (11) at the pulse width of 80 ns and $T=90$ K. For the same operation condition, the excess carrier densities of different devices with lengths of 100 and 50 μm are n_{ex} (100 μm)$=1.6\times10^{18}$ cm^{-3} and n_{ex} (50 μm)$=2.6\times10^{18}$ cm^{-3}, respectively. Now it is clear that the excess carrier density increases as reducing the length of a device as expected from the change of the theoretical survival rate on the device length shown in Table I.

B. Gain of a Gunn laser

The material gain generally includes the energy uncertainty of the electronic states. In order to account for the uncertainty, the integration can be performed over all transition energies weighted by the Lorentzian line shape function $L(h\nu_0-E_{21})$.[22] E_{21} indicates the energy transition from the state of conduction band to one of valence band. The gain including line shape broadening is given by[22]

$$g(h\nu_0)=\int g_{max}(E_{21})(f_2-f_1)L(h\nu_0-E_{21})dE_{21}, \tag{13}$$

where the respective Fermi levels of conduction and valence band are $f_2=1/[e^{(E_1-E_{Fv})/kT}+1]$ and $f_1=1/[e^{(E_2-E_{Fc})/kT}+1]$. E_1, E_2, E_{Fv}, and E_{Fc} are the states and quasi-Fermi levels in the valence and conduction bands, respectively. The maximum gain $g_{max}(E_{21})$ is defined by several material parameters as

$$g_{max}(E_{21})=\frac{\pi e^2\hbar}{n\varepsilon_0 cm_0^2}\frac{1}{h\nu_{21}}|M_T(E_{21})|^2\rho_r(E_{21}), \tag{14}$$

where $M_T(E_{21})$ is the transition matrix element,[23] $\rho_r(E_{21})$ is the reduced density of state for the bulk GaAs,[24] and n is the refractive index. The generation of excess carriers, directly associated with stimulated emission, inverts the carrier population near the band edge, and changes the Fermi level difference of f_2-f_1.[25] The peak of the gain spectrum shifts to the higher photon energies with increasing the excess carrier density.[26] It is because $g_{max}(E_{21})$ has a square root dependence on energy via $\rho_r(E_{21})$.

Excess carrier density n_{ex} increases with reducing the device length L because the exponential term, i.e., the survival rate improving in a short device,[27] is dominant in decision of n_{ex}, as shown in Eq. (11). The shift of the gain peak to high energy levels in Fig. 5 means that the excess carrier density existing at the band edge becomes smaller and hence lasing efficiency is reduced. In shorter devices where the domain size is comparable with the device length, the average electron temperature will be significantly higher than the

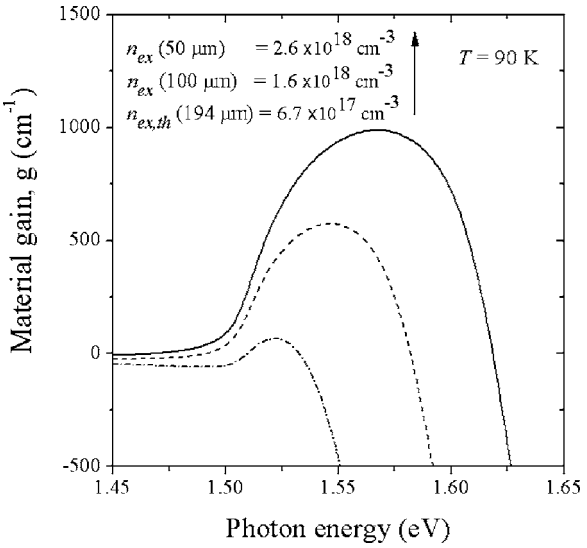

FIG. 5. Excess carrier density dependence of GaAs gain profile at T =90 K.

lattice temperature forcing the nonequilibrium carrier distribution to higher energies and suppressing the population inversion, as shown by us previously.[28] The increase in electron temperature suggests that lack of the experimental observation of lasing in devices with the reduced lengths, i.e., 50 and 100 μm, may indeed be due to the carrier depletion from the lower energy states. Therefore, it is explicit that the reduction of the length, hence higher survival rate and excess carrier density in the whole energy band, is not by itself sufficient to increase the gain. However significant population inversion contributing to strong band-to-band emission may be expected in small devices with two-dimensional structure including a quantum well. It is due to high excess carrier density at the band edge resulting from steeper band edge profile of the density of state in the quantum well.[29]

V. CONCLUSION

The emission characteristics from Gunn devices placed in Fabry-Pérot cavity depend on the device length. For devices having lengths of 200 μm–1 mm, lasing has been observed when the device is biased above the NDR threshold, whereas for devices having small lengths of 100 or 50 μm, only the spontaneous emission is present at all fields. No lasing sign from the devices with small lengths are confirmed by experimental results, indicating that the electron temperature increases with reducing the device length. The improved differential gain and physical durability of a Fabry-Pérot Gunn device can be achieved by the design of a quantum well structured device and heat sink, aiming at increasing band edge excess carrier density contributing to stimulated emission and dissipating Joule heat efficiently, respectively. This would promise the improved lasing with strong stimulated emission and high operation temperatures.

[1]P. D. Southgate, J. Appl. Phys. **38**, 4589 (1967).
[2]P. D. Southgate, IEEE J. Quantum Electron. **QE-4**, 179 (1968).
[3]B. L. Gelmont and M. S. Shur, Electron. Lett. **6**, 531 (1970).
[4]V. Yu. Sudzilovskii, Sov. Phys. Semicond. **7**, 462 (1973).
[5]V. M. Arutyunyan and A. G. Varosyan, Sov. Phys. Semicond. **11**, 167 (1977).
[6]N. Balkan and M. Hostut, Physica B **272**, 291 (1999).
[7]M. Hostut, Ph.D. thesis, The University of Essex, 1999.
[8]S. Chung, A. Boland-Thomas, J. Y. Wah, N. Balkan, and B. K. Ridley, Semicond. Sci. Technol. **19**, S400 (2004).
[9]S. Chung, A. Boland-Thomas, J. Y. Wah, N. Balkan, B. K. Ridley, and J. S. Roberts, Phys. Status Solidi C **2**, 3010 (2005).
[10]S. Chung and N. Balkan, IEE Proc.: Optoelectron. **153**, 84 (2006).
[11]S. Chung and N. Balkan, Appl. Phys. Lett. **86**, 211111 (2005).
[12]B. K. Ridley, Semicond. Sci. Technol. **3**, 542 (1988).
[13]B. K. Ridley, New Sci. **300**, 352 (1964).
[14]P. P. Bohn and G. J. Herskowitz, IEEE Trans. Electron Devices **ED-19**, 14 (1972).
[15]J. T. Verdeyen, *Laser Electronics*, 3rd ed. (Prentice Hall, New Jersey, 1995), p. 152.
[16]R. N. Hall, Proc. Inst. Electr. Eng., **106B**, 923 (1960).
[17]D. K. Schroder, *Semiconductor Material and Device Characterization* (Wiley, New York, 1990), p. 361.
[18]Y. P. Varshni, Phys. Status Solidi **19**, 459 (1967).
[19]S. M. Sze, *Physics of Semiconductor Devices* (Wiley, New York, 1981), p. 850.
[20]S. Chung, Ph.D. thesis, The University of Essex, 2005.
[21]L. A. Coldren and S. W. Corzine, *Diode Lasers and Photonic Integrated Circuits* (Wiley, New York, 1995), p. 39.
[22]L. A. Coldren and S. W. Corzine, *Laser Diodes and Photonic Integrated Circuits* (Wiley, New York, 1995), p. 131.
[23]C. Hermann and C. Weisbuch, Phys. Rev. B **15**, 823 (1977).
[24]L. A. Coldren and S. W. Corzine, in *Laser Diodes and Photonic Integrated Circuits* (Wiley, New York, 1995), p. 125.
[25]D. T. F. Marple, J. Appl. Phys. **35**, 1241 (1964).
[26]B. O. Seraphin and H. E. Bennett, in *Semiconductors and Semimetals*, edited by R. K. Willarson and A. C. Beer (Academic, New York, 1967), Vol. 3, p. 499.
[27]W. W. Chow, S. W. Koch, and M. Sargent III, *Semiconductor-Laser Physics* (Springer-Verlag, Berlin, 1994), p. 95.
[28]N. Balkan and M. Hostut, Physica B **272**, 291 (1999).
[29]P. S. Zory, *Quantum Well Lasers* (Academic, San Diego, 1993), Chap. 1.